科技资料

Computer Modeling and Simulation of Manufacturing Processes

MD-Vol. 20
PED-Vol. 48

COMPUTER MODELING AND SIMULATION OF MANUFACTURING PROCESSES

presented at
THE WINTER ANNUAL MEETING OF
THE AMERICAN SOCIETY OF MECHANICAL ENGINEERS
DALLAS, TEXAS
NOVEMBER 25–30, 1990

sponsored by
THE MATERIALS DIVISION AND
THE PRODUCTION ENGINEERING DIVISION, ASME

edited by
B. SINGH
LAKEHEAD UNIVERSITY
Y. T. IM
KOREAN ADVANCED INSTITUTE OF SCIENCE AND TECHNOLOGY
I. HAQUE
CLEMSON UNIVERSITY
C. ALTAN
UNIVERSITY OF OKLAHOMA

THE AMERICAN SOCIETY OF MECHANICAL ENGINEERS
United Engineering Center • 345 East 47th Street • New York, N.Y. 10017

ISBN No. 0-7918-0566-2

Library of Congress
Catalog Number 90-55953

FOREWORD

In recent years, there has been a phenomenal increase in the use of computational methods for engineering applications. Computer modeling and simulation has emerged as a new field, which promises to have a major impact on research, design, manufacturing, and education. Practicing engineers and researchers are beginning to recognize computer simulation as a cost-effective and convenient way to solve complex problems encountered in the understanding and optimization of manufacturing processes and systems. Along with the growth of hardware capabilities of computers, substantial progress has been made, particularly in the last decade, in the development and application of efficient and robust numerical techniques to problems related to materials processing and manufacturing processes. However, much of this information is scattered in various journals and proceedings. Thus, the timing appeared to be right for a symposium to discuss the problems related to manufacturing processes from the common viewpoint of researchers involved in computer modeling and simulation.

This volume contains the papers presented at the Symposium on Computer Modeling and Simulation of Manufacturing Processes, held in Dallas, November 25–30, 1990. The purpose of this symposium is to provide a forum for the discussion and dessemination of new ideas and to stimulate research in computer modeling and simulation of materials processing and manufacturing. It is hoped that the volume will be of lasting value to researchers and educators in the field of manufacturing engineering.

The editors wish to thank the authors, reviewers, and session chairman and vice chairman for their time and effort.

B. Singh
Y. T. Im
I. Haque
C. Altan

CONTENTS

FINITE ELEMENT MODELING OF ORTHOGONAL METAL CUTTING

K. Komvopoulos[1]
Dept. Mechanical Engineering
University of California
Berkeley, California

S. A. Erpenbeck
Dept. Mechanical and Industrial Engineering
University of Illinois at Urbana-Champaign
Urbana, Illinois

ABSTRACT

The finite element method was used to model chip formation in orthogonal metal cutting. Emphasis was given on the effect of important factors, such as plastic flow of the workpiece material, friction at the tool-workpiece interface, and tool wear geometry, on the cutting process. To simulate separation of the chip from the workpiece, superposition of two nodes at each nodal location of a parting line of the initial mesh was imposed. According to the developed algorithm, the superimposed nodes were constrained to assume identical displacements until approaching to a specified small distance from the tool tip. At that juncture, the displacement constraint was removed and separation of the nodes was allowed. Under the usual plane strain assumption, quasi-static finite element simulations of orthogonal metal cutting were performed for interfacial friction coefficients equal to zero, 0.15, and 0.5 and unworn or worn (cratered) tools having a strongly adhered built-up edge. To investigate the significance of the deformation of the workpiece material on the cutting process, elastic-perfectly plastic and elastic-plastic with isotropic strain hardening and strain rate sensitivity constitutive laws were used in the analysis. For simplicity, the tool material and the built-up edge were modeled as perfectly rigid. In all cases analyzed, the cutting speed and depth of cut were set equal to 183 m/min and 1.27 mm, respectively. Experiments confirmed that cutting of AISI 4340 steel with ceramic-coated tools under these conditions led to the development of a built-up edge and formation of continuous chips. The dimensions of the crater assumed in the finite element simulations involving a cratered tool were also determined from the same cutting experiments. Spatial distributions of the equivalent total plastic strain and the von Mises equivalent stress corresponding to steady-state cutting conditions and the normal and shear stresses at the rake face are contrasted and interpreted qualitatively in terms of critical parameters. The influence of interfacial friction, metal flow characteristics, and tool wear at the rake face on the steady-state magnitude of the cutting forces, shear plane angle, chip thickness, and chip-tool contact length are also elucidated. Several aspects of the metal cutting process predicted by the finite element model agreed well with experimental results and phenomenological observations.

NOMENCLATURE

D	=	material parameter in equation (1)
E	=	elastic modulus
F_n	=	cutting force component perpendicular to the direction of the tool motion
F_p	=	cutting force component parallel to the direction of the tool motion
K_i	=	tangent stiffness matrix at the i^{th} iteration
P	=	normal force at a finite element node
P_0	=	negative pressure
PTOL	=	force tolerance for convergence

[1] Formerly Assistant Professor of Mechanical Engineering, Department of Mechanical and Industrial Engineering, University of Illinois at Urbana-Champaign, Urbana, IL 61801.

$\mathbf{R}$ = vector of applied loads
$\mathbf{R}_i^c$ = vector of load corrections
S = shear force at a finite element node
TOL = parameter controlling node release
$\mathbf{U}_i$, $\mathbf{U}_{i+1}$ = displacement increment vectors at i and i+1 iterations of a loading step
c = clearance tolerance
k = stiffness in stick
l_c = chip-tool contact length
m = material parameter in equation (1)
n = plastic-to-elastic modulus ratio
t = depth of cut
t_c = chip thickness
u_x, u_y = displacements
v = cutting speed
w = width of cut
x, y = cartesian coordinates
Δt = time period of simulation
$\Delta\mathbf{U}_{i+1}$ = vector of incremental displacement corrections
Δx = total horizontal displacement of nodes of boundary ABC
α = rake angle
$\dot{\varepsilon}_p$ = plastic strain rate
ε_p^{eq} = equivalent total plastic strain
μ = coefficient of friction
ν = Poisson's ratio
σ = minimum stress for strain hardening at a constant value of n
σ_{ef} = effective stress at non-zero strain rate
σ^{eq} = von Mises equivalent stress
σ_n = normal stress at the chip-tool interface
σ_s = shear stress at the chip-tool interface
σ_Y = static yield stress
ϕ = primary shear plane angle

INTRODUCTION

Cutting is one of the most frequently used manufacturing processes for producing parts of desirable dimensions. Despite its broad use, the basic mechanics aspects of the process are not clearly understood yet, primarily due to the complex phenomena and the interdependence of controlling process parameters. Early theoretical analyses were based on simple models such as the shear-angle approach (Piispanen, 1948; Merchant, 1945; Oxley, 1962) and the slip-line field theory which assumes rigid-perfectly plastic material behavior (Lee and Shaffer, 1951; Kudo, 1965). To account for variation in the flow stress during cutting, the ideal theory of plasticity was extended to include the effect of work hardening (Palmer and Oxley, 1959). It was reported, however, that machining of materials possessing notably different strain hardening rates did not produce appreciable differences in the cutting forces and chip thickness-to-depth of cut ratio, but the plastic zone was wider for the material exhibiting a higher rate of strain hardening (Oxley et al., 1961). Although these studies provided useful insight to the cutting process, they are based on oversimplistic assumptions and, thus, cannot account for important features, such as frictional interactions at the chip-tool interface, strain hardening, strain rate sensitivity, built-up edge development, chip formation and curling, reported in various investigations (Trent, 1988a; Doyle et al., 1979; Kaneeda et al., 1983; Heginbotham and Gogia, 1961; Cook et al., 1954; Lee, 1984).

With the development of numerical methods such as the finite element technique and the advent of digital computers, computational difficulties and model limitations were overcome and several recent analyses produced elucidating results. One of the first finite element analysis of metal cutting was presented by Klamecki (1973) who treated the incipient chip formation process using a three-dimensional formulation. Later, Usui and Shirakashi (1982) developed a finite element model which accounted for chip formation at steady-state cutting conditions. However, the analysis greatly relied on empirical data and was limited to a rate-independent deformation behavior. Stevenson et al. (1983) used the results from the high strain rate torsion tests of Stevenson and Cleland (1981) to express the flow stress under adiabatic conditions in terms of the strain rate and reported temperature results. Moreover, Iwata et al. (1984) published a finite element analysis of orthogonal metal cutting which utilized an approximate friction law, but it was limited to very low cutting speeds and strain

rates and assumed rigid-plastic deformation. Because this deformation model does not account for elastic deformation, residual stresses cannot be predicted based on this analysis. More recently, Hablanian (1984) obtained finite element solutions corresponding to isothermal conditions by approximating the steady-state mesh configuration, and Strenkowski and Carroll (1985) published finite element results pertaining to the steady-state chip geometry and residual stresses and strains in orthogonal metal cutting. They assumed a temperature-dependent constitutive model and calculated the temperature by assuming adiabatic heating conditions. To overcome difficulties associated with excessive distortion of the finite elements with Lagrangian formulations, an Eulerian-based finite element model of orthogonal cutting with a constitutive model identical to that of the previous investigation was developed (Carroll and Strenkowski, 1988). However, a simple strain rate-independent material behavior was assumed in the latter two studies.

Thus, the review of the literature indicated that further improvement of the basic finite element modeling assumptions and procedures is imperative before an in-depth understanding of the mechanics of metal cutting can be obtained. For example, most of the previous analyses used simple models for constitutive behavior, e.g., rigid-plastic and non-hardening material behavior, or empirical models depending on experimental data, and/or ignored interfacial friction. In fact, no previous study analyzed the effect of the tool wear geometry on the cutting process. The main objective of this investigation, therefore, was to develop a comprehensive finite element analysis of orthogonal metal cutting which is in agreement with the phenomenological observations and simulates the main features of the process fairly accurately. In this paper, the basic aspects of cutting, which have also been incorporated in the model, will be briefly discussed and the details of the modeling procedures will be eluded. Subsequently, results of various simulations will be presented and contrasted to reveal the role of critical parameters in the cutting process.

BASIC ASPECTS OF CUTTING AND PROBLEM DEFINITION

Metal cutting occurs by a process of semi-controlled fracture, in which a very hard and rigid tool moves through the workpiece material along a fixed path (Kaneeda et al., 1983). This process is represented schematically in Fig. 1(a). However, no matter how sharp the cutting edge is, it still appears blunt in comparison to the atoms of the workpiece material. Thus, the actual tool tip geometry can be configured schematically as shown in Fig. 1(b). The material directly in front of the tool tip experiences predominantly large compressive stresses and, thus, it is pushed back leading to the formation of a built-up edge (BUE). The material undergoing fracture at the tip of the BUE flows plastically over the rake face of the tool forming a chip. Because of the typically small rake angle, very high normal stresses are imposed on the workpiece material. Under these conditions, the workpiece material shears along a plane or a thin zone (primary shear zone) where the shear stress is maximum (zone AB in Fig. 1(b)). As oncoming material enters the shear zone, it deforms plastically by a process consisting of dislocation motion leading to material strain hardening.

The significantly work hardened chip flows upwards the tool rake face where large normal and frictional stresses are produced. The large frictional stresses at the tool face often exceed the yield strength of the chip material resulting in seizure at the chip-tool interface. The continuing motion of the bulk of the chip relative to the seized interface creates a zone of intense localized shear

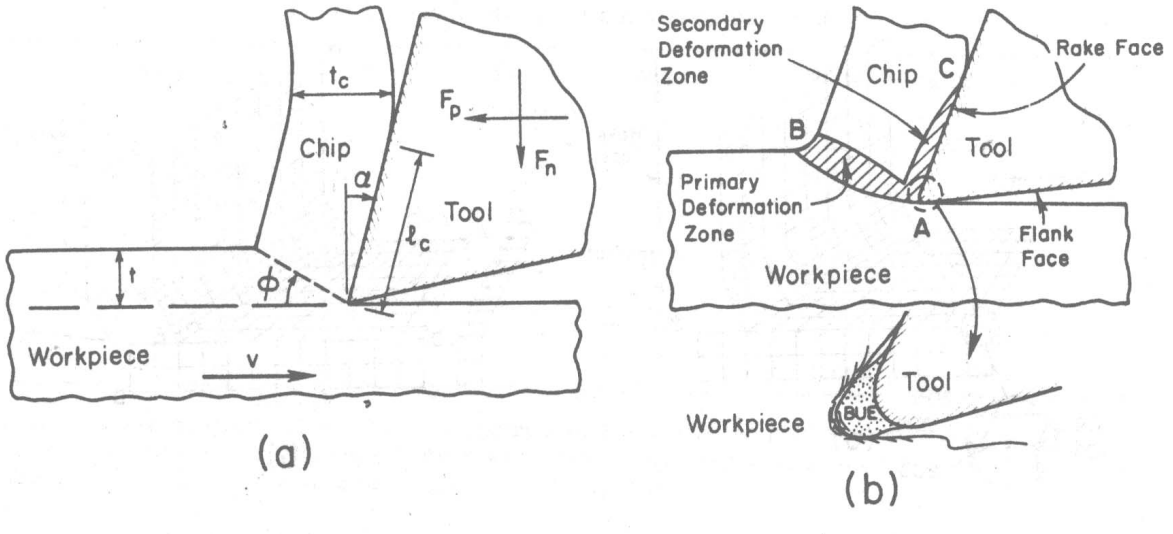

Fig. 1 Two-dimensional representation of the orthogonal metal cutting process: (a) conventional model and pertinent nomenclature; (b) geometry and deformation zones

strain adjacent to the tool face, the so-called secondary shear zone (zone AC in Fig. 1(b)).

To understand the conditions at the chip-tool interface, knowledge of the distribution of the stresses over the chip-tool contact zone is essential. Shearing of the workpiece material at the primary shear plane and plastic flow of the chip over the contact zone generate compressive and shear stresses at the interface. While relationships between cutting forces and important parameters were reported in several investigations, information about the variation of the stresses at the contact zone is sparse.

Despite the extensive research done in metal cutting, the interfacial conditions between the tool and workpiece material remain a controversial subject. Much of this controversy may be attributed to the fact that interfacial conditions vary significantly depending on the cutting parameters and the affinity of the tool to interact with the workpiece. It has been argued, for example, that seizure involving both mechanical and metallurgical bonds occurs over the majority of the contact area (Trent, 1988b). Moreover, machining tests using transparent sapphire tools showed that relative movement at the tool tip occurs despite the high normal pressure and intimate contact (Doyle et al., 1979; Wright, 1981). While the interfacial conditions near the tool tip is yet an unresolved issue, most researchers have similar views with regard to the interfacial conditions at the end of the contact zone. At this region, the pressure is reduced significantly and conventional sliding of the chip over the tool commences.

From the foregoing discussion on the basic aspects of metal cutting, it becomes apparent that development of analytical models which may lead to closed form solutions is extremely difficult, if not impossible, and especially cumbersome due to the highly complex deformation phenomena. Hence, numerical techniques such as the finite element method are effective alternative methods of solution for such difficult problems. The aim of this study, therefore, was to develop a finite element model which accounts for the most essential features observed in actual cutting, such as those shown in Fig. 1(b). Particular emphasis was given to incorporating in the model important parameters such as strain hardening and strain rate sensitivity effects, interfacial friction, tool wear geometry, and BUE formation. The effect of each of these parameters on cutting was critically examined in light of the resulting deformed configuration of the workpiece medium, the stress/strain fields, the distribution of the interfacial stresses, and the variation of the cutting forces, shear angle, chip thickness, and contact length under the various cutting conditions simulated in this study.

FINITE ELEMENT MODELING PROCEDURE

Finite Element Mesh and Modeling Assumptions

The initial finite element mesh configuration and tool geometry are shown in Fig. 2(a). The discontinuous curve reveals the assumed modification of the rake face in the metal cutting analysis with a worn (cratered) tool. The crater dimensions were extracted from microscopy measurements obtained from high speed machining experiments with zero rake angle tools and cutting conditions resembling those in orthogonal cutting. (Results from this work will be presented in a future publication.) Thus, to compare the finite element results with the findings of the experimental study and because of the large number of cutting parameters, orthogonal cutting with a tool having a zero rake angle was selected for analysis. To reduce the computational time, an initial chip geometry was

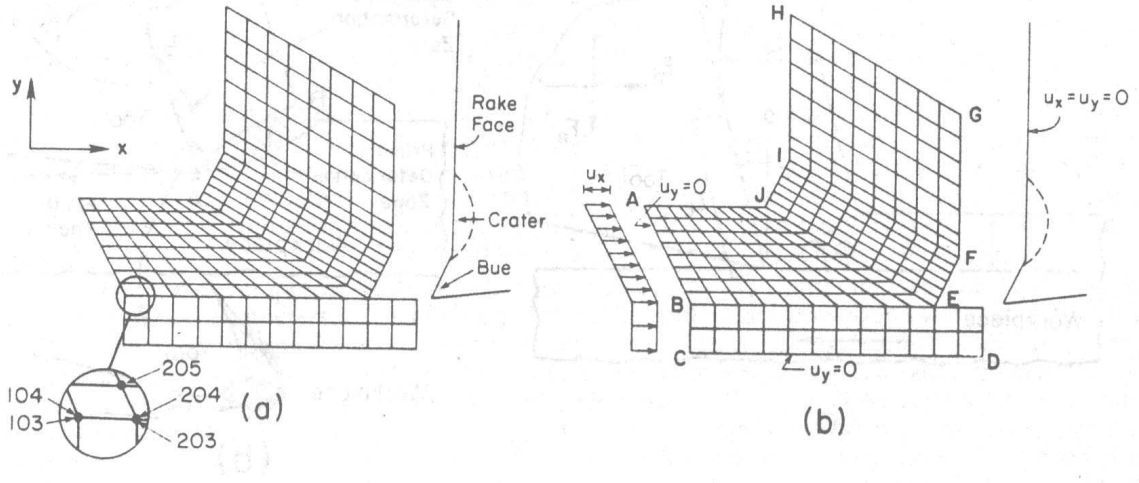

Fig. 2 Undeformed configurations of finite element model showing: (a) nodes of parting line and tool geometry; (b) designation of boundary lines and boundary conditions

incorporated in the finite element mesh. This was based on preliminary estimates of the shear angle and chip thickness resulting under cutting conditions similar to those considered in this investigation. The adopted mesh is an arrangement of 208 isoparametric, 4-node, plane strain elements and 23 line, 2-node, interface elements placed on BEFG (Fig. 2(b)). The total number of nodes is 255 and the integration scheme for the 4-node quadrilateral elements was 2 x 2.

Throughout the analysis, the nodes of the boundaries ABC and CD were constrained against displacement in the y-direction. Simulations of the cutting process were performed by fixing the tool surface and subjecting the nodes on ABC to the same displacement in the x-direction, u_x, as shown in Fig.2(b). This was accomplished in an incremental fashion over a period of time, Δt, which was determined by dividing the total horizontal displacement, Δx, with the cutting speed, v. The cutting speed is an important parameter in the solution procedure, particularly when the deforming workpiece material exhibits strain rate sensitivity effects.

For simplicity, the usual two-dimensional plane strain condition was assumed. This is a reasonable assumption provided the width of cut, w, is notably larger than the depth of cut, t (e.g. $w \geq 5\ t$). In view of the significantly high elastic modulus of most tool materials, a perfectly rigid tool was modeled. This is also an acceptable approximation since elastic deflection of the tool is secondary relatively to the excessive plastic deformation of the workpiece. Furthermore, the idealized case of isothermal cutting conditions, a continuous chip formation process, and a stationary perfectly rigid BUE strongly adhered to the tool tip were assumed. It is well established that the formation of continuous or discontinuous chips and the size of the BUE depend on the cutting speed and the workpiece material. In this analysis, the cutting speed was assumed to be equal to 183 m/min (600 ft/min), the depth of cut was set equal to 1.27 mm (0.05 in), and the workpiece material was assumed to be of AISI 4340 steel. For this value of the cutting speed, the corresponding time Δt is equal to about 9.18×10^{-5} seconds. These values of the cutting parameters and workpiece material are the same with those used in recent experiments with ceramic tools in which machining of AISI 4340 steel under such conditions was found to yield continuous chips and formation of a BUE at the tool tip. The development of a small, stationary, and work hardened BUE which is adhered to the tool tip has been reported in numerous machining processes. Although high speed machining and low ductility workpiece materials generally promote formation of a relatively small BUE, quantitative information about the dependence of the size of the BUE on friction, for the cutting conditions considered in this study, is not available at the present time. Nonetheless, it may be postulated that high friction, e.g. friction coefficient values greater than unity, arising when the workpiece material exhibits an increased propensity to strongly adhere to the tool surface, should result in a larger BUE. Due to the lack of conclussive information regarding the functional relationship between the size of the BUE and the friction coefficient and because of the relatively small range of friction coefficient values considered in this study, the size of the BUE was fixed for all friction conditions considered.

Constitutive Deformation Laws for Workpiece Material

To quantify the effect of the plastic flow characteristics of the workpiece material on the cutting process, elastic-perfectly plastic (EPP) and elastic-plastic with isotropic strain hardening and strain rate sensitivity (EPHSR) constitutive models were considered in the analysis. Table 1 lists the material parameters describing each model which are similar to those reported for isothermal uniaxial

Table 1 Elastic and plastic material parameters

Material Model	Elastic Parameters		Plastic Parameters	
	E (GPa)	ν	σ (MPa)	n
Elastic-perfectly plastic (EPP)	207	0.3	414	0.0
Elastic-plastic with isotropic strain hardening and strain rate sensitivity (EPHSR)	207	0.3	414	0.0498
			517	0.013
			759	0.00183
			1100	0.0

tensile conditions (Lee, 1984). The parameter n in Table 1 is the plastic-to-elastic modulus ratio which represents the coefficient of linear work hardening and depends on the stress range. The strain rate dependency of a material may be approximated as

$$\dot{\varepsilon}_p = D\left(\left(\frac{\sigma_{ef}}{\sigma_Y}\right) - 1\right)^m \qquad \text{for } \sigma_{ef} > \sigma_Y \qquad (1)$$

where $\dot{\varepsilon}_p$ is the plastic strain rate, σ_{ef} is the effective stress at a non-zero strain rate, σ_Y is the static (zero strain rate) yield stress, and D and m are material parameters which are indicative of the strain rate sensitivity and can be determined from experiments. In view of the limited data available for the latter parameters at strain rates representative of machining, i.e. of the order of 10^4 to 10^6 s^{-1}, the data reported by Stevenson and Cleland (1981) were considered to be suitable to the metal cutting problem under consideration. Based on these data and a curve fitting procedure, the values of the material parameters D and m of equation (1) were found equal to 2.21 x 10^5 s^{-1} and 2.87, respectively (Hablanian, 1984).

Simulation of Chip Formation

For a given constitutive behavior model and fixed cutting conditions, the evolution of plasticity in the workpiece is controlled by the relative position of the tool. Chip separation ultimately must involve fracture at a material point of the separation path when plastic deformation becomes maximum. Since accumulation of plastic deformation at a point strongly depends on its relative distance from the tool tip, a plausible criterion for chip separation can be developed based on either a distance tolerance or a critical deformation parameter indicative of the extent of plasticity. Strenkowski and Carroll (1985) adopted the latter approach to account for material separation when an arbitrarily selected value of the effective plastic strain was reached at the pair of nodes closest to the tool tip. While varying the specified strain limit did not influence appreciably the chip geometry and tool forces, the effect on the residual stresses in the chip and cut workpiece was especially profound. Consequently, it was suggested that caution should be exercised in selecting a proper strain value.

In view of the uncertainty regarding the appropriate value of the strain criterion and because information about the dependence of the residual stresses on important parameters was one of the main objectives of this investigation, the somewhat analogous approach of the distance tolerance criterion was invoked to simulate chip separation. A similar technique was used by Usui and Shirakashi (1982) who introduced a ficticious wedge at the tool tip, defined by a tolerance, to allow for smooth chip separation to occur. In this study, simulation of chip formation was done by incorporating a "parting" line BE in the initial mesh configuration (Fig. 2(b)) which consisted of pairs of superimposed nodes, e.g., nodes 103 and 104, 203 and 204, etc., as shown in Fig. 2(a), allowing thus the mesh to separate along this line. Initially, the overlapping nodes were constrained to assume identical displacements in both the x- and y- directions until attaining a specified small distance (tolerance) from the tool tip, TOL. Basically, when a pair of overlapping nodes assumed a distance from the tool tip equal to or less than the magnitude of TOL, the imposed constraint was relaxed and the nodes were allowed to move independently. It should be pointed out that a finite tolerance of sufficient magnitude is essential for avoiding convergence problems arising due to excessive distortion of the finite elements closest to the tool tip. Alternatively, the magnitude of TOL should be small enough in order for the gap at the tool tip to be of minimal size and the error on the steady-state response characteristics of the chip to be practically insignificant. In essence, the magnitude of TOL depends on the element size and can be reduced by refining locally the finite element mesh. Based on the findings of preliminary simulations with various TOL values, a fixed tolerance value equal to one-half of the x-dimension of the elements, i.e. 35 μm, was used throughout this study.

The tool was modeled as a perfectly rigid surface. The built-up edge on the tool tip was assumed to be a stationary deposit of highly work hardened material and, for simplicity, it was considered to be an integral part of the tool. Modeling of a crater on the rake face was accomplished by modifying the geometry of the tool according to optical measurements of the crater dimensions (e.g., depth and average width) obtained from worn ceramic tools having a zero rake angle. Tool-workpiece interaction along the parting line BE and the chip interface EFG (Fig. 2(b)) was accounted for by means of the 2-node interface elements.

Modeling of Tool-Workpiece Contact Interactions

Interactions at the tool-workpiece interface were analyzed by means of the interface elements which control contact behavior by transmitting normal pressure and frictional stresses at those interfacial regions where contact is established. The element parameters for detecting contact between the chip and the tool are the negative pressure, P_0, and the clearance tolerance, c. The mesh nodes of the workpiece may move toward the rigid-tool surface to a distance equal to or less than the specified clearance tolerance. At that juncture, it is assumed that contact was established and, thus, boundary nodal forces are applied. The produced normal forces are equal to those necessary to prevent further displacement toward the tool surface. The clearance tolerance in all simulations was set equal to zero. The pressure parameter P_0 can be used to study sticking between the tool and workpiece material, a phenomenon commonly encountered in metal cutting. In view of the uncertainty regarding the magnitude of this parameter for sticking behavior, it was decided to use the default value of zero negative pressure.

Modeling of interfacial friction was based on Coulomb's law. Localized stick or slip along the tool-workpiece interface depend on the magnitude of the friction coefficient, μ, which constitutes an input parameter of the interface elements. To evaluate the role of friction on the cutting process, the friction coefficient was set equal to zero, 0.15, and 0.5. Thus, depending on the magnitude of the normal and shear (friction) forces at each node, P and S, respectively, one of the following conditions may prevail

$$|S| < \mu P \qquad \text{(stick)} \tag{2a}$$

$$|S| = \mu P \qquad \text{(slip)} \tag{2b}$$

The sign of the friction force in equations 2(a) and 2(b) depends on the relative motion of the workpiece material on the tool surface and is such that the force S is opposed to the direction of sliding. In addition to the friction coefficient, a stiffness in stick parameter, k, was also used. In essence, this is an elastic parameter which is used for transmitting a nodal shear force of magnitude less than the friction limit, i.e. the expected normal force multiplied by the friction coefficient. The stiffness in stick was determined by dividing the expected limit of the friction force with a small relative displacement allowed to occur before localized sliding commences. In this investigation, an empirical approach consisting of several trial and error runs was adopted to yield an estimate for k. In this technique, the magnitude of the parameter k was successively increased until the ratio of the resulting normal and friction nodal forces at the tool-workpiece interface attained a value equal to the specified value of the friction coefficient. Based on this iterative method, a value of the stiffness in stick equal to 1.0×10^{14} Pa was obtained.

Solution Procedure

The general purpose finite element program ABAQUS (Hibbitt, Karlsson and Sorensen, 1988) and an updated Lagrangian formulation were used to solve the metal cutting problem. Since the elements of the finite mesh of the workpiece undergo large plastic deformation and rigid body motion, the stiffness matrix depends on the current geometry and the stress history imposed by the loading sequence. The resulting finite element matrix equations can be expressed as

$$\mathbf{K}_i \Delta \mathbf{U}_{i+1} = \mathbf{R} + \mathbf{R}_i^c \tag{3a}$$

and

$$\mathbf{U}_{i+1} = \mathbf{U}_i + \Delta \mathbf{U}_{i+1} \tag{3b}$$

where $\mathbf{K}_i$ is the tangent stiffness matrix evaluated using the geometry at the i^{th} iteration, $\Delta \mathbf{U}_{i+1}$ is the vector of unknown incremental displacement corrections, $\mathbf{R}$ is the vector of applied loads, $\mathbf{R}_i^c$, is the vector of load corrections, and $\mathbf{U}_{i+1}$, $\mathbf{U}_i$ are the displacement increment vectors at the i+1 and i iterations of a loading step, respectively. Equations (3a) and (3b) are solved iteratively while $\mathbf{K}_i$, $\mathbf{U}_{i+1}$, and $\mathbf{R}_i^c$ are continuously updated until the equilibrium condition is satisfied. To accomplish the desired total loading, an incremental procedure which allows for automatic adjustment of the increment size based on the convergence rate, i.e. nodal force equilibrium, was adopted. In this technique, a specified convergence tolerance, PTOL, which is the tolerance measure for the solution of the equilibrium equations at each increment, was used. Basically, the magnitude of all nodal forces (except those with prescribed displacements) must be equal to or less than PTOL for convergence to be assumed. Typically, the value of PTOL is set equal to a small fraction of a characteristic (or expected) force value. In all the performed finite element simulations, the magnitude of PTOL was set equal to 500 N, which is less than one percent of the expected force values for a unit width of cut.

The solution procedure comprised of two steps. In the first step, contact between the tool surface and the original mesh was established by displacing horizontally the nodes on ABC by a total distance of 13 μm. In the subsequent step, the cutting process was modeled by moving incrementally the nodes on ABC a total horizontal distance of about the size of four elements (i.e. approximately 307 μm) or less, depending on the convergence rate. The maximum number of increments in the second step was 200 and in each increment a maximum of ten iterations was allowed. Table 2 summarizes the important input parameters used in the finite element modeling of chip formation and contact between the tool and the workpiece media.

Finite Element Simulations

Finite element analysis of the orthogonal metal cutting process was comprised of a total of five different simulations. Each simulation was based on different modeling considerations such as the constitutive law of the workpiece material, the magnitude of the interfacial friction coefficient, and

Table 2 Parameters used in the finite element model

Parameter	Magnitude
TOL (μm)	35
P_0 (N)	0
c (μm)	0
μ	0, 0.15, 0.5
k (Pa)	1.0×10^{14}
PTOL (N)	500

the tool wear geometry. This facilitated the analysis and interpretation of the basic aspects of the cutting process and the evaluation and comparison of the associated characteristic parameters (e.g., cutting forces, chip-tool interaction length, curling of the chip, etc.). Table 3 summarizes the main features of the five simulations. The computations were performed on a Convex C210 computer system.

Table 3 Summary of finite element simulations

Simulation	Material Constitutive Model	Friction Coefficient	Tool Geometry
1	EPP	0.0	unworn + BUE
2a	EPHSR	0.0	unworn + BUE
2b	EPHSR	0.15	unworn + BUE
2c	EPHSR	0.50	unworn + BUE
3	EPHSR	0.15	cratered + BUE

RESULTS AND DISCUSSION

Representative results from the quasi-static finite element simulations listed in Table 3 are presented and contrasted in this section for the purpose of enlightening the effect of the plastic flow behavior of the workpiece material, the interfacial friction conditions, and the tool wear geometry on the orthogonal metal cutting process. In particular, deformed finite element meshes revealing the chip flow characteristics and spatial distributions of the equivalent total plastic strain, ε_p^{eq}, and the von Mises equivalent stress, σ^{eq}, in the workpiece and chip material are given. Moreover, results elucidating the variation of the normal, σ_n, and shear, σ_s, stresses at the chip-tool interface are interpreted in terms of important parameters and the estimated steady-state values of the cutting forces parallel and perpendicular to the direction of the tool motion, F_p and F_n, respectively, the shear angle at the primary shear deformation zone, ϕ, the chip thickness, t_c, and chip curl behavior, and the chip-tool contact length, l_c, are analyzed and compared with those deduced from turning tests with AISI 4340 steel under cutting conditions similar to those assumed in this study.

Effect of Workpiece Plastic Flow Behavior

Finite element data obtained from simulation 1 (Table 3) are presented first for the purpose of establishing a reference base of comparison. The undeformed (discontinuous lines) and deformed (continuous lines) meshes resulting at various stages of simulation of the cutting process of an elastic-perfectly plastic workpiece material and for the ideal case of a frictionless interface ($\mu = 0$) are shown in Fig. 3. In this figure, as well as in subsequent figures showing deformed meshes, the magnification factor is equal to one, i.e. the deflections are not exaggerated, but they represent the calculated actual displacements of the chip and workpiece media. The deformed meshes provide a qualitative assessment of the expected physical behavior in orthogonal metal cutting, e.g., shear flow localization and curling of the chip. Examination of Figs. 3(a), 3(b), and 3(c) shows the time history of the process and the progressive development of a primary shear zone extending from the tip of the BUE to the free surface of the workpiece where the chip begins to turn up. Inspection of Fig. 3(c) shows that although the direction of the steady-state shear zone differs from that assumed in the

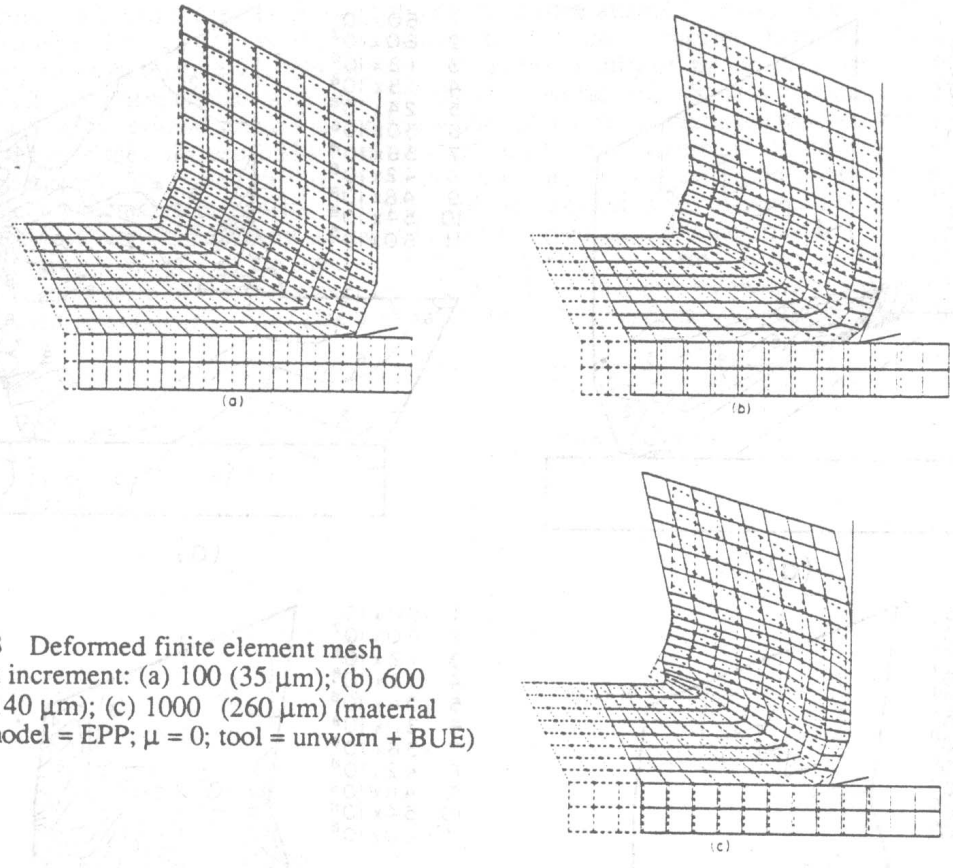

Fig. 3 Deformed finite element mesh at increment: (a) 100 (35 μm); (b) 600 (140 μm); (c) 1000 (260 μm) (material model = EPP; μ = 0; tool = unworn + BUE)

undeformed mesh, the original chip thickness did not change significantly. Although the magnitude of the shear angle and the chip thickness in the undeformed mesh may exhibit a profound effect on the convergence rate and the computational time required for attaining steady-state cutting conditions, the effect on the steady-state solution should be negligibly small. In this simulation, approximately 1000 increments were completed in about 6 hours of cpu time. Although a total distance equal to the length of about four elements was specified, Fig. 3(c) shows that the assumed total distance is equal to about the size of three elements. That the analysis was prematurely terminated is solely attributed to convergence problems, as a consequence of which an automatic incremental reduction of the time increment to a minimum specified limit (about 9.5×10^{-18} seconds in this simulation) resulted in a smaller total displacement of the mesh. Nevertheless, as it will be shown later (e.g., see Figs. 4 and 5), the very small difference between the solutions corresponding to the deformed meshes of Figs. 3(b) and 3(c) confirmed that steady-state conditions were assumed. Another result worthy of considering is the deformation in the chip due to interaction with the tool surface. In contrast to the experimental evidence, Fig. 3(c) shows that shear flow of the chip material adjacent to the interface is minimal, in relation to that encountered in the primary shear zone, evidently due to the zero friction assumption. It is also important to point out the effect of the BUE on the interfacial plastic flow characteristics of the forming chip. In reference to Fig. 3(c), the slope of the finite elements interacting with the BUE is opposite to the slope of the elements sliding on the rake face, i.e., the material at the chip interface is subjected to negative and positive shear strains. A similar result was obtained in the case of material hardening when μ = 0 or 0.15 (e.g., see Figs. 7, 11, and 19), but not when μ = 0.5 (e.g. see Fig.15). Although these findings suggest that under the zero or low friction condition the resulting shear flow characteristics at the chip interface are primarily due to the assumed BUE geometry, further modeling is required in order to quantify the dependence of the interfacial deformation behavior on the friction coefficient and the shape and/or size of the BUE.

Iso-strain and iso-stress contours of the equivalent total plastic strain and von Mises stress corresponding to the deformed mesh configurations shown in Fig. 3 are presented in Figs. 4 and 5, respectively. The distribution of the plastic strain at various stages of cutting shown in Fig. 4 sheds light to the development and orientation of the primary shear zone and the accumulation of plasticity as steady-state conditions are assumed. As expected, the strain is higher (in the range 1.6 to 2.0) at the region where the workpiece turns upward, a result of excessive distortion of the elements (e.g. see also Fig. 3(c)). In view of the magnitude and spatial variation of the strain contours shown in Fig. 4(c), it may be concluded that under the assumed cutting conditions the maximum plastic strain

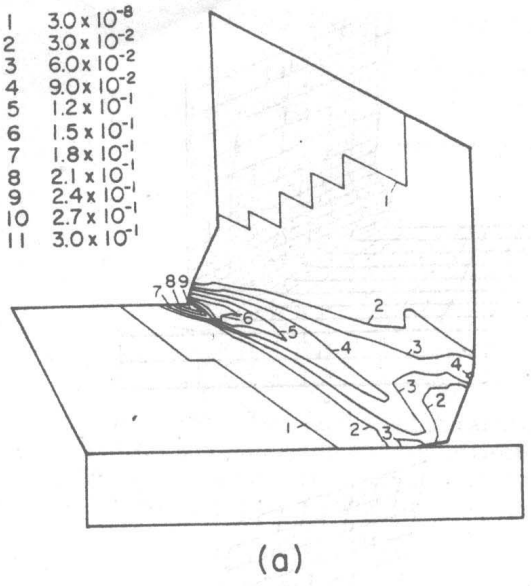

(a)

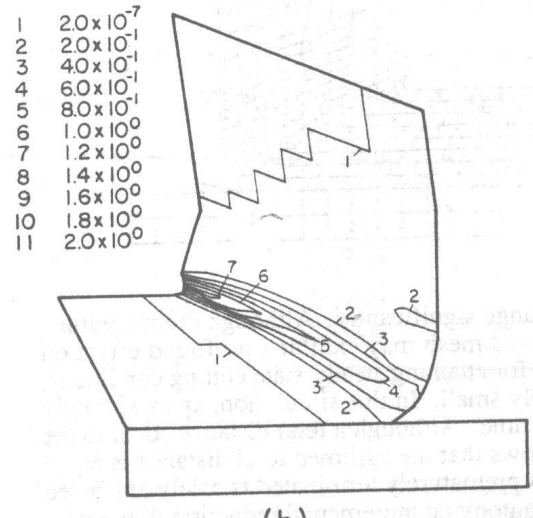

(b)

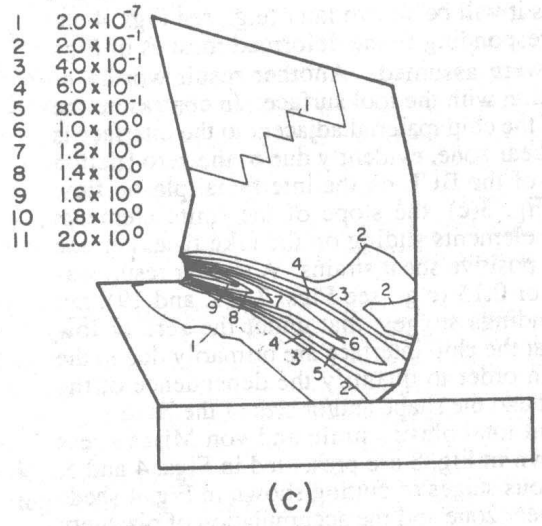

(c)

Fig. 4 Variation of ε_p^{eq} at increment: (a) 100 (35 μm); (b) 600 (140 μm); (c) 1000 (260 μm) (material model = EPP; μ = 0; tool = unworn + BUE)

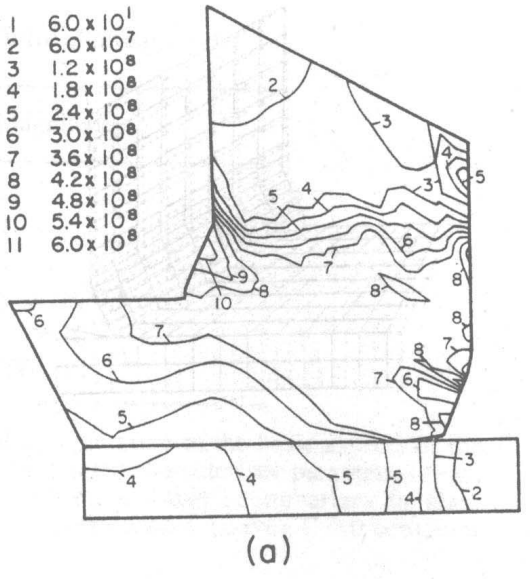

(a)

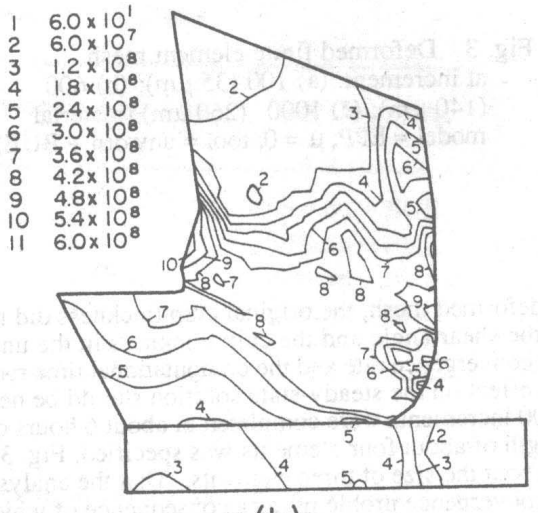

(b)

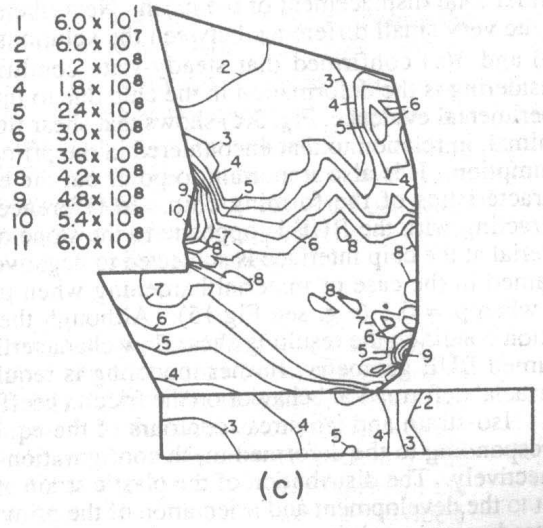

(c)

Fig. 5 Variation of σ^{eq} at increment: (a) 100 (35 μm); (b) 600 (140 μm); (c) 1000 (260 μm) (material model = EPP; μ = 0; tool = unworn + BUE; stress units = Pa)

occurring at the central region of the primary shear zone attains a magnitude between 1.0 and 1.4. Furthermore, the variation of the von Mises stress in the workpiece material, shown in Fig. 5, demonstrates that relatively higher stresses arise in the vicinity of the primary shear zone and at the chip interface where contact with the BUE and the rake face occurs. It is also important to note the development of residual stresses at and below the surface of the produced new workpiece and in the upper mesh of the chip, especially near the chip-tool interface where unloading due to curling of the chip occurred. The small difference of the magnitude and distribution of the strain and stress components plotted in Figs. 4(b), 4(c), 5(b), and 5(c), as well as the magnitude of the corresponding cutting forces, verify that steady state was indeed assumed after 600 increments.

Figure 6 is a plot of the steady-state distribution of the normal stress arising at the tool rake face. The variation of the stress over the rake face is in qualitative agreement with experimentally determined stress distributions (Usui et al., 1984). However, the plot shows stress fluctuations,

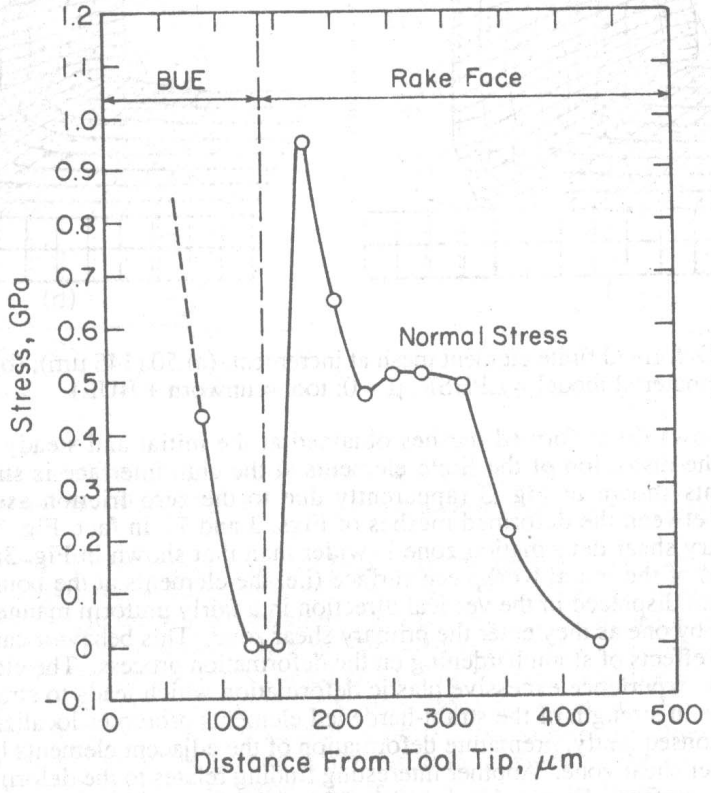

Fig. 6 Distribution of σ_n stress component on tool surface (material model = EPP; $\mu = 0$; tool = unworn + BUE)

especially at the transition region between the BUE and the rake face, which presumably would not be expected in actual cutting. The stress fluctuations can be related to the presence of a small gap at the tip of the BUE, resulting due to discretization of the parting line and separation of the chip according to the adopted node release criterion, and further up the tool surface, i.e. at the boundary of the BUE and the rake face, where because of the irregular geometry, contact between the chip and the tool is not well established (e.g., see also Figs. 3(b) and 3(c)). Thus, the stress distribution on the rake face should be more representative of the actual cutting process and, in fact, it is in fair qualitative agreement with experimental results. Apparently, further mesh refinement or use of higher order elements at the chip interface, in conjunction with a smaller value of the parameter TOL and smoothing of the corners on the tool surface, should yield a smoother stress profile in Fig. 6 (and subsequent similar figures) and, in addition, a relatively gradual change of the stress at those locations where the slope of the rigid surface, i.e. the local effective rake angle, changes abruptly. It should be denoted, moreover, that the formation of a gap at the tip of the BUE may also be attributed to the ideal assumption of a frictionless interface. This is supported by the results obtained in the case of $\mu = 0.5$ (e.g. see Fig. 15).

Figures 7 through 10 show results from the metal cutting simulation in which the workpiece material was assumed to exhibit an elastic-plastic with isotropic strain hardening and strain rate sensitivity behavior and the friction coefficient at the chip-tool interface was set equal to zero (simulation 2a in Table 3). As a result of the relatively large increment size, tolerated in the analysis